NIH Public Access
Author Manuscript
J Immunol. Author manuscript; available in PMC 2016 March 01.

Published in final edited form as:
J Immunol. 2015 March 1; 194(5): 2128–2139. doi:10.4049/jimmunol.1401952.

An Essential Role for RGS Protein/Gα_{i2} Interactions in B Lymphocyte Directed Cell Migration and Trafficking

Il-Young Hwang[1], **Chung Park**[1], **Kathleen Harrison**[1], **Cedric Boularan**[1,2], **Céline Galés**[2], and **John H. Kehrl**[1,3]

[1]Laboratory of Immunoregulation, National Institute of Allergy and Infectious Diseases, National Institutes of Health, Bethesda, MD 20892

[2]Inserm U1048, Institut des Maladies Métaboliques et Cardiovasculaires, I2MC, 1, avenue Jean-Poulhès, BP84225, 31432 Toulouse Cedex 4, France

Abstract

Chemokines engage B lymphocyte surface receptors triggering heterotrimeric G-protein Gα_i subunit guanine nucleotide exchange. RGS proteins limit the duration that Gα_i subunits remain GTP bound, and the loss of an individual RGS protein typically enhances chemokine receptor signaling. Here, we show that B cells carrying a G$\alpha_{i2}^{G184S/G184S}$ mutation that disables all RGS protein/Gα_{i2} interactions exhibit an unexpectedly severe reduction in chemokine receptor signaling. The G$\alpha_{i2}^{G184S/G184S}$ B cells have markedly elevated basal calcium levels, but poor chemokine induced increases; enhanced non-specific migration, but extremely poor chemotaxis. In striking contrast, the G$\alpha_{i2}^{G184S/G184S}$ B cells exhibited enhanced sensitivity to Sphingosine 1-Phosphate (S1P). S1P elicited heightened intracellular calcium responses and enhanced S1P-triggered cell migration. Mice with the G$\alpha_{i2}^{G184S/G184S}$ mutation displayed excessive numbers of germinal center-like structures; abnormal serum immunoglobulin profiles; and aberrant B lymphocyte trafficking. These findings establish an essential role for RGS proteins in B cell chemoattractant signaling and for the proper position of B lymphocytes in lymphoid organs.

Keywords

Sphingosine-1 phosphate (S1P); chemotaxis; trafficking; chemoattractants; intravital; proliferation; RGS proteins; heterotrimeric G-proteins

Signaling downstream of chemoattractant receptors regulates the retention and egress of B lymphocytes from the bone marrow and mediates the trafficking of B cells through most lymphoid organs by controlling entrance, egress, and positioning (1). It also facilitates the interactions of B cells with other cell types and recruits B cells to the skin, inflammatory sites, and isolated lymphoid follicles. The major chemoattractant receptors known to influence B cell behavior are CXCR4, CXCR5, CCR6, CCR7, CCR9, CCR10, S1PR1, S1PR3, CNR2, and GPR183 (2–10). All these receptors are G-protein coupled (GPCR) that

[3]Corresponding author. Mailing address: Laboratory of Immunoregulation, National Institute of Allergy and Infectious Diseases, National Institutes of Health, Bldg 10, Room 11B08, 10 Center Dr MSC 1876, Bethesda, MD 20892; Phone: 301-402-4852. Fax: 301-402-0070. jkehrl@niaid.nih.gov.

NIH-PA Author Manuscript
NIH-PA Author Manuscript
NIH-PA Author Manuscript

NIH-PA Author Manuscript

NIH-PA Author Manuscript

NIH-PA Author Manuscript

use $G\alpha_i$ to link to downstream effectors. Engagement of chemoattractant receptor triggers receptor/heterotrimeric G-protein coupling, $G\alpha_i$ subunit GDP-GTP exchange, functional $G\alpha_i$ dissociation from $G\beta\gamma$ subunits, downstream effector activation, and directed migration (11). Since $G\alpha_i$ subunits possess an intrinsic GTPase activity, GTP hydrolysis facilitates re-assembly of the heterotrimeric G- protein causing signaling to cease. By dramatically accelerating the intrinsic GTPase activity of $G\alpha_i$ subunits, RGS proteins reduce the duration that $G\alpha_i$ subunits remains GTP bound, thereby decreasing effector activation by reducing available $G\alpha_i$-GTP and free $G\beta\gamma$ (12).

The most important parameter that determines cellular responses following exposure to a GPCR ligand is the ability of the ligand to trigger an active receptor conformation (13). An active receptor engages a heterotrimeric G-protein and promotes α subunit nucleotide exchange. Several cell-specific parameters also strongly correlate with G-protein activation including in rank order: G-protein concentration, Gα GTPase activity, and receptor expression level. Non-intuitively small variations in these cell-specific parameters can profoundly affect signaling output (13). Each of these parameters has been implicated in the control of lymphocyte chemokine responsiveness. B cells express an abundance of $G\alpha_{i2}$ and $G\alpha_{i3}$. Yet the loss of one *Gnai2* allele decreases B lymphocyte chemotaxis to CXCL12, CXCL13, and CCL19, particularly so, at low ligand concentrations. The loss of both *Gnai2* alleles profoundly reduces chemotaxis while the loss of both *Gnai3* alleles has a minimal effect (1, 14). Whether $G\alpha_{i2}$ plasma membrane levels undergo physiologically relevant regulation is unknown, however suggesting that they may, $G\alpha_{i2}$ is subject to ubiquitination and proteasomal degradation (15). The HIV Nef protein specifically targets this system to degrade $G\alpha_{i2}$ in Nef expressing lymphocytes, thereby reducing lymphocyte chemokine responsiveness (16). The second parameter, the rate that Gα subunits hydrolyze GTP to GDP is an intrinsic property of individual G-proteins, but as indicated above this rate is subject to regulation by RGS proteins. Most RGS proteins enhance the GTPase activity of $G\alpha_i$ and $G\alpha_q$, but not that of $G\alpha_s$ or $G\alpha_{12/13}$ (12). Reduced expression levels of RGS1, RGS3, RGS10, RGS13, and RGS16 have all been shown to enhance responsiveness to chemoattractants (17–21). Conversely, overexpression of an individual RGS protein generally reduces chemoattractant sensitivity. Arguing that RGS1/$G\alpha_{i2}$ levels help control lymphocyte chemokine sensitivity the impact of the loss of an allele of *Gnai2* is alleviated by the loss of an allele of *Rgs1* (14). The third parameter, receptor expression level, has been shown to help control B cell positioning in lymphoid organs. The ratio between CXCR5 and CCR7 expression determines whether a B cell localizes in the lymph node (LN) follicle or at the T cell zone- follicle interface (8). Increased GPR183 expression re-localizes B cells in the spleen and LNs and the ratio between CXCR4 and CXCR5 expression helps germinal center (GC) B cell traffic between light and dark zones (9, 10, 22).

Determining the role of an individual RGS protein in lymphocyte function has been assessed by gene targeting in mice, however an overall assessment of their role in B and T lymphocytes remains elusive because of the multiple family members. For example, murine follicular B cells express *Rgs2, Rgs3, Rgs10, Rgs14, Rgs18*, and *Rgs19* mRNAs while GC B cells have a different pattern of RGS protein expression (23). They have higher levels of *Rgs2* and *Rgs10*, lower levels of *Rgs14, Rgs18*, and *Rgs19*, and the additional expression of

NIH-PA Author Manuscript

NIH-PA Author Manuscript

NIH-PA Author Manuscript

Rgs1, Rgs9, and *Rgs13* (23). Mapping the site of interaction of RGS proteins with $G\alpha_i$ proteins provided a solution to this problem of multiple family members. A single mutation in $G\alpha_i$ proteins renders them insensitive to RGS proteins as it abrogates RGS protein binding (24). This mutation has no effect on $G\alpha_i$ binding to receptors, $G\beta\gamma$, or effectors; and no effect on $G\alpha_i$ expression. Mice with a mutation in the *Gnai2* locus ($G\alpha_{i2}^{G184S/G184S}$) have been made. Previous study of these mice has revealed defects in neutrophil trafficking, enhanced platelet aggregation, abnormal cardiac function, and central nervous system dysfunction (25–30). Because of the dominant role $G\alpha_{i2}$ plays in B lymphocyte chemoattractant responses, these mice are an attractive model to assess the importance of RGS proteins in chemoattractant signaling in B cells. To avoid the impact of the $G\alpha_{i2}$ mutation on non- hematopoietic cell types, we have largely studied B cells from mice reconstituted with bone marrow cells from mice with the $G\alpha_{i2}^{G184S}$ mutation. Contrary to expectations, B cells from these mice were hyposensitive to CXCL12, CXCL13, and CCL19, yet they were hyper-responsive to sphingosine 1- phospate (S1P). Our data indicates that the cellular RGS proteins help to coordinate B cell sensitivity to chemoattractants and in their absence B cells no longer properly interpret environmental chemoattractant cues resulting in abnormal B cell positioning and trafficking.

Material and Methods

Mice and bone marrow reconstitutions

C57BL/6 and B6.SJL-Ptprc^a Pepc^b/BoyJ mice were obtained from Jackson Laboratory. *Gnai2*$^{G184S/G184S}$ mice were each backcrossed more than 17 times on to C57BL/6. For those experiments that directly compared wild type and G184S KI mice, littermate control were always used. The KI mice were bred as heterozygotes. For bone marrow reconstitution, twenty seven weeks old B6.SJL-Ptprc^{a}Pepc^b/BoyJ (CD45.1) mice were irradiated twice with 550 rads for total of 1100 rads and received bone marrow from C57BL/6 CD45.2 mice (control) or from *Gnai2*$^{G184S/G184S}$ CD45.2 mice. Mixed chimeric mice were made by reconstituting twenty irradiated CD45.1 mice with a 1:1 mix of bone marrow from C57BL/6 CD45.1 mice (WT) and from *Gnai2*$^{G184S/G184S}$ CD45.2 mice. The engraftment was monitored by sampling the blood 28 days later. The mice were used 6–8 weeks after reconstitution. All mice were used in this study were 6–14 weeks of age. Mice were housed under specific-pathogen-free conditions. All the animal experiments and protocols used in the study were approved by the NIAID Animal Care and Use Committee (ACUC) at the National Institutes of Health.

Cells

Splenic B cells were isolated by negative depletion using biotinylated antibodies to CD4, CD8, Gr-1 (Ly- 6C and Ly 6G), and CD11c and Dynabeads M-280 Streptavidin (Invitrogen) as previously described (1). The B cell purity was greater than 95%. When needed B cells were cultured in RPMI 1640 containing 10% fetal calf serum (FCS, Gibco), 2 mM L-glutamine, antibiotics (100 IU/mL penicillin and 100 μg/mL streptomycin), 1 mM sodium pyruvate, and 50 μM 2-mercaptoethanol. Cell culture media for S1P chemotaxis was same as above except charcoal-dextran filtered FCS was used.

NIH-PA Author Manuscript

NIH-PA Author Manuscript

NIH-PA Author Manuscript

Standard flow cytometry and cell proliferation

Single cells were re-suspended in PBS, 2% FBS, and stained with fluorochrome-conjugated or biotinylated antibodies against B220 (RA3-6B2), IgD (11-26c-2a), IgM (R6-60.2), CD24 (M1/69), CD3 (145-2C11), CD4 (GK1.5), CD5 (53-7.3), CD8 (53-6.7), CD11c (HL3), CD11b (M1/70), CD138 (281–2), CD19 (1D3), CD38 (90), IgG1 (X56), CD93 (AA4.1), BP-1 (6C3), GL-7 (GL-7, Ly-77), CD95 (Jo2), CD21 (4E3), CD23 (B3B4), CD43 (S7), CD184 (CXCR4, 2B11), CXCR5 (2G8), CCR7 (4B12), CD11a (M17/4), CD49d (9C10, MFR4.B), CD54 (YN1/1.74), CD62L (MEL-16), CD45.1 (A20), or CD45.2 (104) (all from eBioscience, Biolegend, or BD Pharmingen). Biotin-labeled antibodies were visualized with fluorochrome-conjugated streptavidin (eBioscience). LIVE/DEAD® Fixable Aqua Dead Cell Stain Kit (Molecular Probes) was used in all experiments to exclude dead cells. Data acquisition was done on FACSCanto II (BD) flow cytometer and analyzed with FlowJo software (Treestar). The cell proliferation studies were performed using the CFSE (Molecular Probes) in a standard dye dilution assay. Purified B cells were stimulated for 96 hours with various combinations of the following reagents: 1 μg/ml CD40 (HM40-3), 1 μg/ml LPS (Sigma-Aldrich), recombinant mouse IL-4 (10 ng/ml, R&D Systems), or 10 μg/ml AffiniPure F(ab')$_2$ fragment goat anti-mouse IgM (Jackson ImmunoResearch Laboratories). Data acquisition was done on FACSCanto II flow cytometer. The percentages of cells that divided and the proliferation indexes were calculated using FlowJo software. The % of cells that divided is the percentage of the cells of the original sample, which divided (assuming that no cells died during the culture). The proliferation index is the total number of divisions divided by the number of cells that went into division, again assuming no cell death.

Intracellular flow cytometry

Cells were intracellular stained using the BD Biosciences Cytofix/Cytoperm Fixation/ Permeabilization Kit protocol using the S1P1 receptor antibody (dilution of 1:100), followed by the secondary donkey anti–rabbit IgG PE conjugated. The cells were re-suspended with 1% BSA/PBS. The S1PR1 antibody (H- 60, Santa Cruz Biotechnology) and phycoerythrin (PE) conjugated donkey anti–rabbit IgG (R&D Systems) were used. Cells analyzed as above.

Chemotaxis assays

Chemotaxis assays were performed using a transwell chamber (Costar) as previously described (1). Splenic B cells were immunostained for B cell subsets with fluorochrome-conjugated antibodies against B220, CD21, CD23, and CD24 washed twice, re-suspended in complete RPMI 1640 medium and added in a volume of 100 μl to the upper wells of a 24-well transwell plate with a 5 μm insert. Lower wells contained various doses of chemokines in 600 μl of complete RPMI 1640 medium. The numbers of cells that migrated to the lower well after 2 h incubation were counted using a MACSQuant flow cytometer (Miltenyi Biotec). The percent migration was calculated by the numbers of cells of a given subset that migrated into the bottom chamber divided by the total number of cells of that subset in the starting cell suspension, and multiplying the results by 100. D-erythro-sphingosine 1-phosphate was purchased from Avanti Polar Lipids. CXCL13, CCL19 and CXCL12 were

NIH-PA Author Manuscript

NIH-PA Author Manuscript

NIH-PA Author Manuscript

purchased (R&D Systems). Fatty acid free bovine serum albumin (FAF-BSA) was purchased (Sigma-Aldrich).

Intracellular calcium measurements

Cells were seeded at 10^5 cells per 100 μl loading medium (RPMI 1640, 10% FBS) into poly-D-lysine coated 96-well black wall, clear-bottom microtiter plates (Nalgene Nunc). An equal volume of assay loading buffer (FLIPR Calcium 4 assay kit, Molecular Devices) in Hank's balanced salt solution supplemented with 20 mM HEPES and 2 mM probenecid was added. Cells were incubated for 1 h at 37 °C before adding chemokine and then the calcium flux peak was measured using a FlexStation 3 (Molecular Devices). The data was analyzed with SOFT max Pro 5.2 (Molecular Devices). Data is shown as fluorescent counts and the y-axis labeled as Lm1.

Immunohistochemistry

Immunohistochemistry was performed using a described method (31). Freshly isolated LNs were fixed in freshly prepared 4% paraformaldehyde (Electron Microscopy Science) and agitated overnight at 4°C. LNs were embedded in 4% low melting agarose (Invitrogen) in PBS and sectioned with a vibratome (Leica VT-1000 S) at a 30 μm thickness. Thick sections were blocked in PBS containing 10% FCS, 1 mg/ml anti-Fcγ receptor (BD Biosciences), and 0.1% Triton X-100 (Sigma) for 30 minutes at room temperature. Sections were immunostained with the following antibodies: anti-B220, anti-CD4, anti-Ki67 (all from eBioscience), anti-CD169 (R&D System), anti-CD21/35 (BioLegend) and agitated overnight at 4°C. Stained thick sections were microscopically analyzed by using a Leica SP5 confocal microscope (Leica Microsystem, Inc.) and images were processed with Leica LAS AF software (Leica Microsystem, Inc.) and Imaris v.7.6.1 (Bitplane).

Homing and egress assays

Purified splenic B cells from *Gnai2*$^{+/+}$, *and Gnai2*$^{G184S/G184S}$ mice were labeled with 1 μM eFluor® 450, or 2.5 μM CMTMR for 15 min at 37°C and equal numbers of viable cells (8–10 million) were injected intravenously into recipient mice. After 2 h, spleen, iLNs, and pLNs were removed and gently dissociated into single cell suspensions. Peripheral blood was collected by retro-orbital eye bleeding. After removing red blood cells with Tris-NH_4Cl, the cells were re-suspended in PBS containing 1% BSA at 4°C. LIVE/DEAD® Fixable Aqua Dead Cell Stain Kit (Molecular Probes) was used to exclude dead cells. Data acquisition was done on FACSCanto II flow cytometer and analyzed with FlowJo software (Tree Star).

Intravital two-photon laser scanning microscopy (TP-LSM)

Inguinal LNs were prepared for intravital microscopy as described (32, 33). Cell populations were labeled for 15 minutes at 37°C with 1 uM green cell tracker CMFDA, 2.5~5 uM red cell tracker CMTMR (Molecular probes). 5–10 million labeled cells of each population in 200 ml of PBS were adoptively transferred by tail vein injection into 6~10-week-old recipient mice. After anesthetizing the mice by intraperitoneal injection of Avertin (300 mg/kg, tribromoethanol, Sigma), the skin and fatty tissue over inguinal LN were removed.

NIH-PA Author Manuscript

NIH-PA Author Manuscript

NIH-PA Author Manuscript

The mouse was placed in a pre-warmed coverglass chamber slide (Nalgene, Nunc). The chamber slide was then placed into the temperature control chamber on the Leica SP5 microscope. The temperature of air was monitored and maintained at 37.0± 0.5°C. Inguinal LN was intravitally imaged from the capsule over a range of depths (10–220 μm). All of Two-photon imaging was performed with a Leica SP5 inverted 5 channel confocal microscope (Leica Microsystems) equipped with 0.95 NA (immersion medium used distilled water). Two-photon excitation was provided by a Mai Tai Ti:Sapphire laser (Spectra Physics) with a 10 W pump, tuned to 810 or 910 nm. Emitted fluorescence was collected using a 4 channel non-descanned detector. Wavelength separation was through a dichroic mirror at 560 nm and then separated again through a dichroic mirror at 495 nm followed by 525/50 emission filter for CMFDA (Molecular probes); a dichroic mirror at 650 nm followed by 610/60 nm emission filter for CMTMR; and the Evans blue signal was collected by 680/50 nm emission filter. Sequences of image stacks were transformed into volume-rendered four-dimensional videos using Imaris software and tracking analysis was transformed by using autoregressive motion algorithm of Imaris software v.7.6.1 (Bitplane).

Immunizations and ELISAs

WT and mutant mice were immunized with either sheep RBCs or TNP-KLH. For the sheep RBC immunizations 2×10^8 sheep RBCs (Lonza Walkerville, Inc.) were given by intraperitoneal injection. TNP-KLH (Biosearch Technology) was mixed with Imject® Alum (Thermo Scientific) and introduced into mice (100 μg) via intraperitoneal injection. Mice were boosted with same dose of antigen at the indicated days along with Alum. Serum TNP specific Ig levels in these mice were analyzed by ELISA. Briefly, 96 well ELISA plates (Nunc) were coated with TNP-BSA (Biosearch Technology) overnight at 4°C, washed and blocked with 1% BSA fraction V (Sigma-Aldrich), serum titers were then added to the plates and incubated 4h at 4°C. After washing alkaline phosphatase-labeled goat anti-mouse Ig isotype specific antibodies were added for 2h at RT (SouthernBiotech). After washing, PNPP one component substrate (SouthernBiotech) was used to detect the amount of secondary antibody bound.

BRET assays

The coding regions for S1PR1, S1PR3, or CXCR4 receptors (Missouri S&T cDNA Resource center) were subcloned into phRLuc (Perkin Elmer). Plasmids encoding YFP tagged $G\alpha_{i1}$, $G\alpha_{i2}$ or $G\alpha_{i3}$ have been previously described (34). $G\alpha_{i2}$ -RLuc8, $G\alpha_{i3}$ -Rluc8, $G\beta_1$ and $G\gamma_2$-GFP2 have also been previous described (35). For the pre-association experiment, HeLa cells were transfected (100 ng/well) with DNA constructs coding for the BRET donor (S1PR1-RLuc, S1PR3-RLuc or CXCR4-Rluc) and increasing (100–1000 ng/well) amounts of the construct coding for BRET acceptor (Gαi1-YFP, Gαi2-YFP, or Gαi3-YFP). One day after transfection the cells were harvested and re-plated in 96-wells microplates, and 24h later the media was replaced by Hanks Buffer Salt Solution and the luciferase substrate coelenterazine h (Promega) added (5 μM). Emitted luminescence and fluorescence were measured simultaneously using the Mithras^{tm} fluorescence-luminescence detector (Berthold Technologies). Cells expressing BRET donors alone were used to determine background. The BRET ratio was calculated as: (emission at 540 nm / emission at 480 nm) after addition of Coelenterazine h. For G protein activation, the indicated constructs

NIH-PA Author Manuscript

NIH-PA Author Manuscript

NIH-PA Author Manuscript

were transiently expressed in HeLa cells. Forty-eight hours after transfection, cells were washed with PBS, detached with PBS and 5 mM EDTA, and re-suspended in PBS with 0.1% (w/v) glucose at room temperature. Cells were then equally distributed in a 96-well microplate (Wallac, PerkinElmer Life and Analytical Sciences) and incubated in the presence or absence of the different ligands for 1 min. BRET2 between *R*Luc8 and GFP2 was measured after the addition of the substrate coelenterazine 400a (5 μM, Interchim). BRET2 readings were collected using a modified Infinite F500 (Tecan Group Ltd). The mBRET signal was calculated by the ratio of emission of GFP2 (510–540 nm) to *R*Luc8 (370–450 nm). Cells expressing BRET donors alone were used to determine background. The results were expressed in delta milli-BRET units (mBRET), 1 delta mBRET corresponding to the BRET ratio multiplied by 1000 for the treated condition minus BRET ratio multiplied by 1000 for control condition.

Immunoblotting

The cells were lysed in a buffer of 20 mM HEPES, pH 7.4, 50 mM β-glycerophosphate, 1 mM Na_3VO_4, 0.5% (vol/vol) Triton X-100, 0.5% (vol/vol) CHAPS (3-[(3-cholamidopropyl)-dimethylammonio]-1- propane sulfonate hydrate), and 10% (vol/vol) glycerol with a protease inhibitor 'cocktail' tablet. The lysates were separated by SDS-PAGE and transferred to nitrocellulose membrane by iBLOT Gel Transfer System (Invitrogen). The membrane was incubated with 5% nonfat milk w/v in TBS buffer (25 mM Tris- HCl, pH 7.5; 150 mM NaCl; 0.1% Tween-20) for 1 h, and then reacted with the primary antibody in TBS buffer with 2.5 % nonfat milk or 5% BSA w/v for overnight by shaking at 4 degree. The appropriated second antibodies conjugated to HRP were used to detect the protein of interest via enhanced chemoluminescence (ECL). The following primary antibodies were used phosphor-p44/42 MAPK (Erk1/2) (Thr202/Tyr204) (E10) mouse mAb #9106, 1:2000; phosospho-Akt (Ser473) (D9E) XP® rabbit mAb #4060, 1:2000; p44/42 MAPK (Erk1/2) antibody #9102, 1:1000; Akt (pan) (11E7) rabbit mAb #4685, 1:1000 (all from Cell Signaling); $G\alpha_{i2}$ antibody (L5): sc-13534, mouse mAb, 1:500 (Santa Cruz). Secondary antibody for rabbit primaries was Goat anti-rabbit IgG (H + L)-HRP conjugate #170- 6515, 1:3000 (BioRad); and for the mouse primaries was horse anti-mouse IgG, HRP-linked antibody #7076, 1:3000, (Cell Signaling).

Statistics

In vivo results represent samples from 3–9 mice per experimental group. Results represent mean values of at least triplicate samples. Standard errors of the mean (SEM) and *p* values were calculated with *t* test or ANOVA using Microsoft Excel software or GraphPad Prism (GraphPad software). *, $p > 0.05$; **, $p > 0.005$; and ***, $p > 0.0005$.

Results

The loss of $G\alpha_{i2}$/RGS protein interactions alters the distribution of B cells in lymphoid organs

Bone marrow from $G\alpha_{i2}^{G184S/G184S}$ knock-in mice (referred to hereafter as G184S KI) or from wild type control mice were used to reconstitute C57BL/6 mice. Approximately 8 weeks after reconstitution some of the mice were immunized with sheep red blood cells

NIH-PA Author Manuscript

NIH-PA Author Manuscript

NIH-PA Author Manuscript

(sRBC) via intraperitoneal (i.p.) injection. Ten days later we assessed the distribution of B cells in various lymphoid organs from both immunized and non-immunized mice. We found an approximately 40% increase in the number of B cells in the spleens of both the non-immunized and immunized G184S KI mice as compared to the spleens from the WT mice (Fig. 1A). In contrast, the numbers of B cells in LNs, Peyer's patches, and the peripheral blood were all significantly reduced in the G184S KI mice (Fig. 1A). However, we found little difference in splenic and bone marrow B cell development with the exception of a modest decrease in Fraction B cells in the bone marrow of the G184S KI mice (Fig. 1B & C). Surprisingly, we noted a consistent increase in the number of B cells with a GC phenotype in the spleens of the non-immunized G184S KI mice (Fig. 1D). These results indicate that B cell development proceeded relatively normally in the G184S KI mice bone marrow and that immature B cells exited the bone marrow and continued their maturation in the spleen. However mature B cell trafficking from the spleen to the blood and into peripheral lymphoid organs was disturbed. The reason for the increase in constitutive GC formation in the spleen was unknown, but had been observed previously in both the *Rgs1* and *Rgs13* deficient mice (17, 36).

The loss of $G\alpha_{i2}$/RGS protein interactions increases non-specific B cell migration, but reduces specific migration to chemokines

Next, we assessed chemoattractant and homing receptor expression on B cells from the wild type and from G184S KI bone marrow reconstituted mice. Shown are individual flow cytometry data and a summary of the evaluation of multiple mice (Fig. 2A & B). Among the different receptors we checked the only significant difference was in the expression of L-selectin (CD62L), which was modestly lower on the G184S KI B cells. This reduction could contribute to a homing defect as CD62L functions to promote the rolling of B cells on high endothelial venules in LNs. The reason for the lower level of CD62L is unclear. B cells lacking both $G\alpha_{i2}$ and $G\alpha_{i3}$ have levels of CD62L similar to that of wild type B cells (1). Next, we used B cells from the 1:1 mixed chimera mice to assess wild type and G184S KI B cells chemotaxis to CXCL12, CCL19, and CXL13; relying on flow cytometry to evaluate the responsiveness of different B cell splenic subsets from the two genotypes simultaneously. The G184S KI B cells from the T1, T2- follicular, and follicular B cells subset had an increase in spontaneous migration, while the spontaneous migration of T2-marginal zone and marginal zone subsets were similar to the WT cells (Fig. 2C). All of the G184S KI B cell subsets responded poorly to each of the chemokines, with little increase noted over the spontaneous migration (Fig. 2C and D). For example the G184S KI follicular B cells required a three- fold higher concentration of CXCL13 to trigger a similar % of specific migration (Fig. 2D). These results indicate that the loss of $G\alpha_{i2}$/RGS protein interactions in B cells results in an enhancement of spontaneous motility, while reducing the capacity of the B cells to sense a chemoattractant gradient.

The G184S KI B cells have an elevated basal intracellular calcium level, but severely blunted chemokine triggered increases

As we typically assess chemotaxis after a two hour exposure to chemoattractant, a more direct measure of chemoattractant receptor signaling and the functional dissociation of $G\alpha$ and $G\beta\gamma$ subunits is an increase in intracellular calcium levels. Following ligand exposure an

NIH-PA Author Manuscript

NIH-PA Author Manuscript

NIH-PA Author Manuscript

increase is detectable within seconds and peaks approximately 45 seconds later. We compared B cells from purified from wild type and G184S KI bone marrow reconstituted mice. Shown are intracellular calcium responses to concentrations of chemokine that elicit optimal or near optimal B cell chemotaxis. In each instance the G184S KI B cells exhibited a slower increase, a reduced peak in intracellular calcium, and a slower return towards basal levels (Fig. 3A). For each chemokine we tested a range of concentrations and plotted the peak intracellular calcium level as a function of the log chemokine concentration (Fig. 3B). The slope of the dose response curve was flatter when we used B cells from the G184S KI mice and there was a substantial reduction in peak intracellular calcium over the range of concentrations tested. We also noted an increase in the basal intracellular calcium level in the G184S KI (not shown in the previous calcium data as it was normalized). The G184S KI B cell basal intracellular calcium level exceeded that of the wild type B cells by nearly 50% (Fig. 3C).

To examine another measure of chemokine receptor signaling we stimulated B cells with CXCL12 for various durations and immunoblotted for the presence of phosphorylated ERK (pERK) and phosphorylated AKT (pAKT). We found little difference in the levels of phosphorylated ERK and AKT in non-stimulated B cells isolated from mice reconstituted with wild type or G184S KI bone marrow (Fig. 3D). However, 1 minute after stimulation we noted a 30–40% reduction in the levels of pERK and pAKT in the G184S KI B cells. We also checked $G\alpha_{i2}$ levels in the resting G184S KI and wild type B cells, which were similar (Fig. 3D). The reduced level of pERK and pAKT at 1 minute after stimulation of the G184S KI B cells is consistent with the reduction in intracellular calcium noted after chemokine stimulation.

The homing of adoptively transferred B cells to LNs provides an *in vivo* measure of B cells adhesion to high endothelial venules and an assessment of their ability to transmigrate across high endothelial venules (33). To test the homing of the genotypic distinct B cells, we adoptively transferred differentially labeled wild type and G184S KI B cells into wild type mice and two hours later assessed their localization (Fig. 3E). We found that the G184S KI B cells accumulated in the blood and inefficiently entered into LNs. The numbers of cells in the spleen were similar to that of wild type. This homing defect helps explain the low numbers of G184S KI B cells in LNs and Peyer's patches.

S1P receptor (S1PR) signaling is enhanced in the G184S KI B cells

The retention of B cells in LNs and their egress into the efferent lymphatics depends upon a delicate balance between signals received from chemokine receptors and S1PRs (37). The predominant receptor controlling B lymphocyte egress from LNs and Peyer's Patches is the type 1 S1PR or S1PR1. The S1PR1 couples to $G\alpha_i$ protein and *Gnai2*$^{-/-}$ B cells migrate poorly to S1P (38). The manipulation of either RGS1 or RGS13 expression in cell lines is known to affect S1P-signaling to downstream effectors (39, 40). To test the impact of the loss of $G\alpha_{i2}$/RGS proteins interactions on S1P receptor signaling, we first verified that wild type and G184S B cell expressed similar levels of S1PR1 (Fig. 4A). Next, we tested S1P mediated increases in intracellular calcium. In contrast, to what we had observed with the different chemokines, S1P triggered a more robust intracellular calcium response in the

NIH-PA Author Manuscript

NIH-PA Author Manuscript

NIH-PA Author Manuscript

G184S KI B cells than in the WT B cells (Fig. 4B). In addition, the initial slope of the calcium curve was similar to that of wild type B cells. Consistent with the signaling data more G184S $B220^+$ cells specifically migrated to S1P better than we observed using wild type cells (Fig. 4C). The G184S $G\alpha_{i2}$ mutation strikingly impacted chemokine and S1P receptor signaling discordantly.

Since the G184S mutation is limited to $G\alpha_{i2}$ a difference in S1PR1 and chemokine receptor coupling to $G\alpha_{i2}$ and $G\alpha_{i3}$ might help explain the discordant results. To investigate this possibility we tested the relative preference of S1PR1 and CXCR4 for $G\alpha_{i2}$ versus $G\alpha_{i3}$ using a bioluminescence resonance energy transfer assay (BRET). BRET saturation curves were generated and used to calculate the mBRET50 for each GPCR/G-protein pair. This provides a measure of the relative affinity between the two proteins. A higher affinity interaction results in a lower mBRET50 (41). In addition we looked at ligand induced changes in BRET as a measure of G-protein activation. This analysis indicated that S1PR1 exhibited a significantly greater tendency to pre-associates with $G\alpha_{i3}$ versus $G\alpha_{i2}$, while CXCR4 had little preference for one G-protein versus the other. However, both ligand bound receptors could efficiency activate either $G\alpha_{i2}$ or $G\alpha_{i3}$ (Fig. 4D). These data indicate that both S1PR1 and CXCR4 can activate $G\alpha_{i2}$, but raise the possibility that the differential pre-association of S1PR1 with $G\alpha_{i3}$ may temper the impact of the G184S $G\alpha_{i2}$ mutation for S1PR1 signaling.

To test whether the G184S $G\alpha_{i2}$ mutation affected B lymphocyte LN egress, we transferred wild type and G184S KI B cells and two hours later administered a CD62L antibody, which will block any further homing of B cells into LNs (33). Eighteen hours later we determined the number of wild type and G184S KI B cells in LNs, the spleen, and in the blood. Since the G184S KI B cells have a homing defect, we corrected the data for the difference in homing showing the results as a ratio between the homing and egress results (Fig. 4E). This analysis shows that fewer G184S KI B cells accumulate in the blood following administration of CD62L. While more G184S KI B cells accumulated in the spleen, there was no statistical difference in the residual number of cells in the LN when corrected for the homing defect. These data indicate that B cell LN egress is not significantly impaired in the G184S KI mice. The tendency of the cells to remain in the spleen may be explained by the increased sensitivity to S1P, which is known to impacts B cell trafficking in the spleen (42).

G184S KI B cells enter poorly into the splenic white pulp and LN follicles, but retain relatively normal in vivo motility

To test B cell localization in spleen and LNs we adoptively transferred differentially labelled wild type and G184S KI B cells and assessed their positioning in LNs and the spleen via immunohistochemistry a day after transfer. In the LN follicles the ratio of wild type to G184S KI B cells was 2.2 while in the T cell zone the ratio was reversed with 0.4 WT B cells present per G184S KI B cell. This indicates that some G184S KI B cells had failed to properly enter into the LN follicle (Fig. 5A). We also found skewed ratios between WT to G184S B cells at different sites in the spleen. The ratios in the B cell zone, T cell zone, and red pulp were 3.3, 0.5, and 0.8, respectively (Fig. 5B). Many G184S KI B cells had failed to enter or remain in the B cell zones in spleen, rather localizing in the red pulp and

NIH-PA Author Manuscript

NIH-PA Author Manuscript

NIH-PA Author Manuscript

occasionally in the T cell zones. Next, we used intravital multiphoton microscopy to check the motility of the wild type and G184S KI B cells in the inguinal LN of wild type mice by adoptively transferring the cells into wild type mice. While there were some statistical differences in the average track displacement, track length, and track speed variability the overall motility pattern of the G184S KI B cells was surprisingly intact (Fig. 5C). Thus despite a major impairment in chemokine gradient sensing, random B cell motility was not significantly affected.

Absent B cell $G\alpha_{i2}$/RGS protein interactions distorts normal LN and splenic architecture

To assess LN and splenic architecture we performed multi-parameter confocal microscopy with antibodies recognizing CD169, B220, CD4, Ki67, and CD21. We assembled multicolor composite images of the inguinal LN and the spleen from mice reconstituted with bone marrow from WT or G184S KI mice. The mice were examined 8–10 weeks after bone marrow reconstitution. The G184S KI bone marrow reconstituted mice had smaller inguinal LNs with sparse, poorly delineated LN follicles. B cells were readily found in the T cell zones (Fig. 6A). The spleens of the G184S KI reconstituted mice were larger and striking disorganized. They had small B cell zones that had GC-like structures in the absence of any exogenous immune challenge. The marginal zone regions of the spleen were poorly delineated from the red pulp. The splenic red pulp contained many more B cells than usual and numerous Ki67 positive cells aligned along the edge of the spleen (Fig. 6B). The spleens of the immunized G184S KI reconstituted mice resembled those of the non-immunized mice although the GC-like structures were larger with numerous Ki67 positive cells. Ki67 is a marker of proliferating cells. While GC B cells are Ki67 positive it is not a specific marker. Many Ki67 positive cells were found in the splenic red pulp in the immunized G184S KI reconstituted mice (Fig.6C and 6D). These results further confirm the importance of controlling $G\alpha_{i2}$ signaling for proper organization of lymphoid organs and raise some questions about the potential roles of $G\alpha_{i2}$ and RGS proteins in impacting B cell proliferative responses.

Enhanced G184S KI B cell proliferation and abnormal humoral immunity in the G184S KI mice

Several older reports had variably implicated Gi proteins in B cell antigen receptor (BCR) and LPS induced B cell proliferation by treating the cells with pertussis toxin, which ADP ribosylates $G\alpha_i$ proteins blocking receptor triggered nucleotide exchange (43, 44). More recent studies using gene targeted mice support a role for $G\alpha_i$ proteins in B cell inductive responses. For example, BCR crosslinking led to a suboptimal elevation of intracellular calcium and a slightly poorer proliferative response in B cells that lacked $G\alpha_{i2}$, while the additional loss of $G\alpha_{i3}$ further diminished B cell responses (1). To test whether the lack of an RGS/protein $G\alpha_{i2}$ interaction affected B cell proliferative responses to inductive signals we stimulated fluorescently labeled B cells and quantitated the % of dividing cells and calculated a proliferative index based on dilution of the fluorescent dye. In these experiments we used B cells from the mixed chimera mice distinguishing the wild type and G184S KI mice based on their expression of CD45.1 versus CD45.2. This allowed us to test the wild type and G184S KI B cells under identical experimental conditions. We found that a greater percentage of B cells from the G184S KI mice divided in response to anti-IgM and

NIH-PA Author Manuscript

NIH-PA Author Manuscript

NIH-PA Author Manuscript

to CD40 stimulation, while a similar percentage responded to LPS. However, only the G184S KI B cells stimulated with anti-IgM had an augmented proliferative index (Fig. 7A). These results suggest that the loss of normal $G\alpha_{i2}$ regulation by RGS proteins lowers the threshold needed for certain signals to trigger B cell division.

Finally, we examined the status of humoral immunity in the G184S KI mice. First, we measured the serum immunoglobulin levels in the wild type and G184S KI mice. Here we tested non-reconstituted mice so the $G\alpha_{i2}$ mutation is not limited to hematopoietic cells. We found that compared to wild type littermate controls the G184S KI mice had elevated levels of IgM, IgG2b, and IgG2c; similar levels of IgG1 and IgA, and a depressed level of IgG3 (Fig. 7B). The most significant difference was in the level of IgG2b, which is typically reflective of antibody producing cells that have originated from GCs. The reduction in IgG3 suggests reduced antibody production by marginal zone and B1 B cells. Second, we immunized mice with the thymus dependent antigen TNP-Keyhole limpet hemocyanin and assessed the TNP specific antibody response at various days following a primary immunization and 7 days after an antigen boost. We found that the G184S KI mice primary IgM, IgG2b, and IgG2c anti-TNP responses slightly exceeded those of the wild type mice, while the primary IgG1 response was similar (Fig. 7C). Following boosting the G184S KI mice had a stronger IgG2b and IgG2c anti-TNP response than did the wild type mice. These results indicate that the B cell trafficking problems in the G184S KI mice had not adversely reduced the quantitative antibody response to a neo-antigen, but rather the mice exhibited features of a chronically activated immune phenotype.

DISCUSSION

Appearing early in eukaryote evolution and expanding with the lineage-specific expansion of Gα subunits, RGS proteins have served as a primary mechanism to regulate the sensing of environmental signals by GPCRs (45). Functionally, RGS proteins accelerate GPCR signaling kinetics and govern receptor sensitivity by accelerating the intrinsic GTPase activity of $G\alpha_i$ and $G\alpha_q$ family members (46). In B lymphocytes, $G\alpha_{i2}$ is the principal heterotrimeric G-protein that links chemokine receptors to downstream effectors to mediate chemokine gradient sensing (1). In the absence of $G\alpha_{i2}$, $G\alpha_{i3}$ marginally substitutes, and the combined loss of $G\alpha_{i2}$ and $G\alpha_{i3}$ is catastrophic for chemokine sensing. While the loss of an individual RGS protein enhances chemokine receptor signaling, here we show that blocking the interactions of the cellular pool of RGS proteins with $G\alpha_{i2}$ results in a severe impairment in B lymphocyte chemotaxis to CXCL12, CXCL13, and CCL19. As a consequence B cells home poorly to LNs and Peyer’s patches; inadequately enter B cell compartments; and tend to accumulate in the splenic red pulp. In contrast, S1P signaling to mobilize intracellular calcium and to trigger B cell chemotaxis was enhanced by the loss of RGS protein mediated regulation of $G\alpha_{i2}$. This may contribute to the homing defect and the tendency of the G184S KI B cells to remain in the splenic red pulp. Several other surprising findings arose from the analysis of the G184S KI mice such as the presence of constitutive splenic GCs, a distorted serum immunoglobulin profile, an enhanced IgG2b and IgG2c response to a booster immunization, and an augmented proliferative response of B cells to BCR crosslinking.

NIH-PA Author Manuscript

NIH-PA Author Manuscript

NIH-PA Author Manuscript

While the chemokine elicited changes in intracellular calcium, ERK, and AKT activation were modestly affected in the G184S KI B cells, chemokine directed cell migration was severely inhibited *in vitro* and *in vivo* B cell trafficking was substantially disrupted. How might the lack of $G\alpha_{i2}$/RGS protein interactions cause such a severe defect in gradient sensing and directed cell migration? Early observations of the cellular effects of RGS proteins on GPCR signaling may provide an answer (47). In these studies RGS proteins accelerated signal onset and as well as accelerated the decay of $G\beta\gamma$-gated ion channel responses. Several models have been proposed to account for these observations. A "physical scaffolding" model argued that the additional domains present in many RGS proteins mediate interactions that modulate receptor/heterotrimeric G-protein coupling, i.e. improve receptor GEF activity (48). However, B-lymphocytes largely express RGS proteins that lack additional domains making this hypothesis unlikely to contribute to the B cell phenotype in the G184S KI mice. Another model, which has recently received additional support, has been termed "kinetic scaffolding" or "spatial focusing" (46, 49). This model proposes that G-protein activation becomes saturated near spatially constrained GPCRs causing GTP hydrolysis to become the rate limiting step in the G-protein cycle rather than GPCR mediated release of GDP from the heterotrimer. RGS proteins enhance steady state pathway activation by providing additional heterotrimer G-proteins for activation reducing the need for GPCRs and heterotrimeric G-proteins to associate by slow diffusion and collision events. Such a "kinetic scaffolding" function of RGS proteins would promote a more rapid onset of chemokine receptor signaling as well as a sharper deactivation. Consistent with this model the G184S KI B cells had a delayed increase in chemokine induced intracellular calcium and a prolonged recovery phase following chemokine challenge. In addition, CXCL12 elicited a delayed increase in phosphorylated ERK and AKT. As chemokine gradient sensing depends on $G\beta\gamma$ signaling and requires the chemokine receptor/G-protein machinery to provide an accurate and rapid intracellular readout of an external chemokine field (50), the failure to properly generate those signals would impair chemokine triggered chemotaxis as we observed.

The loss of RGS proteins often enhances the sensitivity of cells to a GPCR agonist, yet the G184S KI B cells had a decreased chemokine induced intracellular Ca^{2+} responses. How can this be explained? The elevated basal calcium and increased spontaneous migration in chemotaxis assays implies a heightened basal level of GPCR signaling in the G184S KI B cells. A similar phenotype was observed in the G184S KI neutrophils (29). The absence of RGS protein/$G\alpha_{i2}$ interactions will enhance signaling from low level GEF activity arising from constitutive GPCR activation and basal levels of endogenous ligands. This signaling could recruit desensitization mechanisms, which tempers subsequent responses to relevant signals. Both experimental studies and theoretical modeling of GPCR signaling pathways have implicated RGS proteins in the regulation of ligand-mediated desensitization (51, 52). Chemokine receptor desensitization is largely thought to be mediated by agonist induced receptor phosphorylation, which promotes the recruitment of nonvisual arrestins, β-arrestin-1 and β-arrestin-2 (53, 54). This uncouples the receptor from the heterotrimeric G proteins, targets the receptor for internalization, and can trigger G-protein-independent signaling. The internalized receptor has two fates: it can be recycled and returned to the cell surface as a resensitized receptor, or it can be sorted to lysosomes for degradation. Yet B

NIH-PA Author Manuscript

NIH-PA Author Manuscript

NIH-PA Author Manuscript

lymphocytes must maintain chemokine sensitivity even in a chemokine-rich environment. RGS proteins by limiting the duration that Gβγ subunits can recruit G-protein receptor kinases may suppress the subsequent engagement of the β-arrestin system helping B cell retain chemokine receptor sensitivity in the presence of low levels of chemokines. When exposed to high concentrations of cognate ligand, RGS proteins become less relevant, as the receptor rapidly becomes phosphorylated and internalized. In studies not shown, CXCR5, CCR7, and CXCR4 were lost at a similar rate from wild type and G184S KI B cells following exposure of the cells to saturating doses of cognate ligand (IYH, unpublished observation).

In contrast to the rightward shift we noted with chemokines, the S1P peak intracellular calcium dose response curve shifted leftward and S1P-mediated chemotaxis was slightly enhanced. How can the loss of the $G\alpha_{i2}$/RGS protein interaction differentially affect chemokine and S1P receptors? The preferential pre-coupling of S1PR1 to $G\alpha_{i3}$ versus $G\alpha_{i2}$, may limit the impact of the $G\alpha_{i2}$ mutation. Uncoupling of the receptor from $G\alpha_{i}$ proteins may be less likely as $G\alpha_{i3}$ is subject to normal RGS protein regulation. Alternatively, RGS proteins may also be functionally more important in regulating the signaling output from chemokine versus S1P receptors. The S1P/S1PR1 axis controls the access of B cells to the lymph and blood as S1P levels are high in the blood and lymph and sharply lower in the lymphoid organs (37). S1P acts over a short range triggering B lymphocyte adhesion, and subsequent endothelial transmigration. Compared to chemokine receptors, S1PR1 engagement triggers poor *in vitro* chemotaxis, and there is little *in vivo* evidence for S1PR1 directed B cell migration (38). Once lymphocytes enter the blood or lymph they are exposed to high concentrations of S1P, which causes rapid S1PR1 internalization. While RGS proteins may temper S1P receptor signaling in lymphoid organs this becomes less relevant once the cell approaches the blood as the receptor is severely downregulated. The implication of our findings is that chemokine receptors need a much more graded response to function properly, while the S1PR1 receptors function more like an on-off switch.

The increase of GC B cells in the spleen despite the reduction in the number of B cells in follicles in the G184S KI mice is also of interest. Both *Rgs1*$^{-/-}$ and *Rgs13*$^{-/-}$ mice have increased numbers of large GCs (17, 36). The reason for the increase is unclear. In the *Rgs13*$^{-/-}$ mice altered CREB signaling may contributed to the phenotype, but in the G184S KI mice RGS protein functions that do not depend on $G\alpha_{i2}$ are not affected. For the same reason a role for RGS proteins in regulating Gq-linked signaling cannot be invoked to account for the constitutive germinal formation. The enhanced signaling to BCR crosslinking noted in the G184S KI mice could contribute as mice that have an increased activity of downstream signaling elements such as Bruton tyrosine kinase (Btk) spontaneously form GCs (55). Furthermore, spontaneous GC formation is a common finding in a variety of autoimmune diseases. GC abnormalities could also arise from subtle B cell trafficking defects in the GC, which are likely present in the G184KI mice. This could alter both the duration of GCs, plasma cell formation, and the production of memory B cells. As other cell types involved in GC formation including CD4 follicular helper T cells and dendritic cells also lack $G\alpha_{i2}$/RGS protein interactions they may also contribute to the phenotypes noted in the G184S KI mice. Further studies using mice with the G184S KI

NIH-PA Author Manuscript

NIH-PA Author Manuscript

NIH-PA Author Manuscript

limited to for example CD4 T cells will be needed to determine if the enhanced spontaneous GCs are B cell intrinsic or secondary to altered function of CD4 T cells or another cell type.

In conclusion, the analyses of mice in which RGS proteins can no longer bind to $G\alpha_{i2}$ have provided new insights into the role of RGS protein in B lymphocytes. The lack of $G\alpha_{i2}$/RGS protein interactions in B cells results in their failure to properly translate the environmental cues, which direct B cell navigation, into the intracellular signals needed to control cell membrane extensions, actin dynamics, and cell motility. As a consequence there is a major loss in gradient sensing and impaired chemokine directed cell migration. In contrast, S1P receptor signaling is enhanced. The different impact of the $G\alpha_{i2}$ G184S mutation on chemokine and S1P receptor signaling may be secondary to the different functional roles of the two receptor systems or to alternative $G\alpha_i$ protein usage. The combined impact is to reduce the entrance of B cells into peripheral lymphoid organs, partial entrapment of B cells in the splenic red pulp, and altered B cell positioning in B cell niches. By providing a rheostat like function and a kinetic scaffold, RGS proteins fine tune the outcome of ligand chemoattractant receptor engagement helping to coordinate chemokine receptor sensitivity and receptor desensitization mechanisms.

Acknowledgements

I-Y.H. and J.H.K designed the study. I-Y.H. performed the majority of the experiments. C.B. and C.G. designed and performed the BRET assays, C.P. performed the intravital imaging, K.H. managed the mice and performed the immunoblotting and ELISAs and J.H.K wrote the manuscript. We would like to thank Dr. Anthony Fauci for his continued support. This research was supported by the intramural program of the National Institutes of Allergy and Infectious Diseases.

References

1. Hwang IY, Park C, Luong T, Harrison KA, Birnbaumer L, Kehrl JH. The loss of Gnai2 and Gnai3 in B cells eliminates B lymphocyte compartments and leads to a hyper-IgM like syndrome. PLoS One. 2013; 8:e72596. [PubMed: 23977324]
2. Ma Q, Jones D, Springer TA. The chemokine receptor CXCR4 is required for the retention of B lineage and granulocytic precursors within the bone marrow microenvironment. Immunity. 1999; 10:463–471. [PubMed: 10229189]
3. Pereira JP, An J, Xu Y, Huang Y, Cyster JG. Cannabinoid receptor 2 mediates the retention of immature B cells in bone marrow sinusoids. Nat Immunol. 2009; 10:403–411. [PubMed: 19252491]
4. Allende ML, Tuymetova G, Lee BG, Bonifacino E, Wu YP, Proia RL. S1P1 receptor directs the release of immature B cells from bone marrow into blood. J Exp Med. 2010; 207:1113–1124. [PubMed: 20404103]
5. Ansel KM, Ngo VN, Hyman PL, Luther SA, Forster R, Sedgwick JD, Browning JL, Lipp M, Cyster JG. A chemokine-driven positive feedback loop organizes lymphoid follicles. Nature. 2000; 406:309–314. [PubMed: 10917533]
6. Forster R, Mattis AE, Kremmer E, Wolf E, Brem G, Lipp M. A putative chemokine receptor, BLR1, directs B cell migration to defined lymphoid organs and specific anatomic compartments of the spleen. Cell. 1996; 87:1037–1047. [PubMed: 8978608]
7. Forster R, Schubel A, Breitfeld D, Kremmer E, Renner-Muller I, Wolf E, Lipp M. CCR7 coordinates the primary immune response by establishing functional microenvironments in secondary lymphoid organs. Cell. 1999; 99:23–33. [PubMed: 10520991]
8. Reif K, Ekland EH, Ohl L, Nakano H, Lipp M, Forster R, Cyster JG. Balanced responsiveness to chemoattractants from adjacent zones determines B-cell position. Nature. 2002; 416:94–99. [PubMed: 11882900]

NIH-PA Author Manuscript

NIH-PA Author Manuscript

NIH-PA Author Manuscript

9. Pereira JP, Kelly LM, Xu Y, Cyster JG. EBI2 mediates B cell segregation between the outer and centre follicle. Nature. 2009; 460:1122–1126. [PubMed: 19597478]
10. Gatto D, Paus D, Basten A, Mackay CR, Brink R. Guidance of B cells by the orphan G protein-coupled receptor EBI2 shapes humoral immune responses. Immunity. 2009; 31:259–269. [PubMed: 19615922]
11. Kehrl JH, Hwang IY, Park C. Chemoattract receptor signaling and its role in lymphocyte motility and trafficking. Curr Top Microbiol Immunol. 2009; 334:107–127. [PubMed: 19521683]
12. Watson N, Linder ME, Druey KM, Kehrl JH, Blumer KJ. RGS family members: GTPase-activating proteins for heterotrimeric G-protein alpha-subunits. Nature. 1996; 383:172–175. [PubMed: 8774882]
13. Kinzer-Ursem TL, Linderman JJ. Both ligand- and cell-specific parameters control ligand agonism in a kinetic model of g protein-coupled receptor signaling. PLoS Comput Biol. 2007; 3:e6. [PubMed: 17222056]
14. Hwang IY, Park C, Harrision KA, Huang NN, Kehrl JH. Variations in Gnai2 and Rgs1 expression affect chemokine receptor signaling and the organization of secondary lymphoid organs. Genes Immun. 2010; 11:384–396. [PubMed: 20508603]
15. Chishiki K, Kamakura S, Yuzawa S, Hayase J, Sumimoto H. Ubiquitination of the heterotrimeric G protein alpha subunits Galphai2 and Galphaq is prevented by the guanine nucleotide exchange factor Ric-8A. Biochem Biophys Res Commun. 2013; 435:414–419. [PubMed: 23665327]
16. Chandrasekaran P, Buckley M, Moore V, Wang LQ, Kehrl JH, Venkatesan S. HIV- 1 Nef impairs heterotrimeric G-protein signaling by targeting Galpha(i2) for degradation through ubiquitination. J Biol Chem. 2012; 287:41481–41498. [PubMed: 23071112]
17. Moratz C, Hayman JR, Gu H, Kehrl JH. Abnormal B-cell responses to chemokines, disturbed plasma cell localization, and distorted immune tissue architecture in Rgs1−/− mice. Mol Cell Biol. 2004; 24:5767–5775. [PubMed: 15199133]
18. Han JI, Huang NN, Kim DU, Kehrl JH. RGS1 and RGS13 mRNA silencing in a human B lymphoma line enhances responsiveness to chemoattractants and impairs desensitization. J Leukoc Biol. 2006; 79:1357–1368. [PubMed: 16565322]
19. Berthebaud M, Riviere C, Jarrier P, Foudi A, Zhang Y, Compagno D, Galy A, Vainchenker W, Louache F. RGS16 is a negative regulator of SDF-1-CXCR4 signaling in megakaryocytes. Blood. 2005; 106:2962–2968. [PubMed: 15998835]
20. Garcia-Bernal D, Dios-Esponera A, Sotillo-Mallo E, Garcia-Verdugo R, Arellano-Sanchez N, Teixido J. RGS10 restricts upregulation by chemokines of T cell adhesion mediated by alpha4beta1 and alphaLbeta2 integrins. J Immunol. 2011; 187:1264–1272. [PubMed: 21705617]
21. Williams JW, Yau D, Sethakorn N, Kach J, Reed EB, Moore TV, Cannon J, Jin X, Xing H, Muslin AJ, Sperling AI, Dulin NO. RGS3 controls T lymphocyte migration in a model of Th2-mediated airway inflammation. Am J Physiol Lung Cell Mol Physiol. 2013; 305:L693–L701. [PubMed: 24077945]
22. Allen CD, Ansel KM, Low C, Lesley R, Tamamura H, Fujii N, Cyster JG. Germinal center dark and light zone organization is mediated by CXCR4 and CXCR5. Nat Immunol. 2004; 5:943–952. [PubMed: 15300245]
23. Boularan C, Kehrl JH. Implications of non-canonical G-protein signaling for the immune system. Cell Signal. 2014; 26:1269–1282. [PubMed: 24583286]
24. Lan KL, Sarvazyan NA, Taussig R, Mackenzie RG, DiBello PR, Dohlman HG, Neubig RR. A point mutation in Galphao and Galphai1 blocks interaction with regulator of G protein signaling proteins. J Biol Chem. 1998; 273:12794–12797. [PubMed: 9582306]
25. Huang X, Fu Y, Charbeneau RA, Saunders TL, Taylor DK, Hankenson KD, Russell MW, D'Alecy LG, Neubig RR. Pleiotropic phenotype of a genomic knock-in of an RGS- insensitive G184S Gnai2 allele. Mol Cell Biol. 2006; 26:6870–6879. [PubMed: 16943428]
26. Signarvic RS, Cierniewska A, Stalker TJ, Fong KP, Chatterjee MS, Hess PR, Ma P, Diamond SL, Neubig RR, Brass LF. RGS/Gi2alpha interactions modulate platelet accumulation and thrombus formation at sites of vascular injury. Blood. 2010; 116:6092–6100. [PubMed: 20852125]

NIH-PA Author Manuscript NIH-PA Author Manuscript NIH-PA Author Manuscript

27. Fu Y, Huang X, Piao L, Lopatin AN, Neubig RR. Endogenous RGS proteins modulate SA and AV nodal functions in isolated heart: implications for sick sinus syndrome and AV block. Am J Physiol Heart Circ Physiol. 2007; 292:H2532–H2539. [PubMed: 17277016]
28. Talbot JN, Jutkiewicz EM, Graves SM, Clemans CF, Nicol MR, Mortensen RM, Huang X, Neubig RR, Traynor JR. RGS inhibition at G(alpha)i2 selectively potentiates 5- HT1A-mediated antidepressant effects. Proc Natl Acad Sci U S A. 107:11086–11091. [PubMed: 20534514]
29. Cho H, Kamenyeva O, Yung S, Gao JL, Hwang IY, Park C, Murphy PM, Neubig RR, Kehrl JH. The Loss of RGS Protein-Galphai2 Interactions Results in Markedly Impaired Mouse Neutrophil Trafficking to Inflammatory Sites. Mol Cell Biol. 2012; 32:4561–4571. [PubMed: 22966200]
30. Talbot JN, Jutkiewicz EM, Graves SM, Clemans CF, Nicol MR, Mortensen RM, Huang X, Neubig RR, Traynor JR. RGS inhibition at G(alpha)i2 selectively potentiates 5-HT1A-mediated antidepressant effects. Proc Natl Acad Sci U S A. 2011; 107:11086–11091. [PubMed: 20534514]
31. Chai Q, Onder L, Scandella E, Gil-Cruz C, Perez-Shibayama C, Cupovic J, Danuser R, Sparwasser T, Luther SA, Thiel V, Rulicke T, Stein JV, Hehlgans T, Ludewig B. Maturation of lymph node fibroblastic reticular cells from myofibroblastic precursors is critical for antiviral immunity. Immunity. 2013; 38:1013–1024. [PubMed: 23623380]
32. Park C, Hwang IY, Kehrl JH. Intravital two-photon imaging of adoptively transferred B lymphocytes in inguinal lymph nodes. Methods Mol Biol. 2009; 571:199–207. [PubMed: 19763968]
33. Park C, Hwang IY, Sinha RK, Kamenyeva O, Davis MD, Kehrl JH. Lymph node B lymphocyte trafficking is constrained by anatomy and highly dependent upon chemoattractant desensitization. Blood. 2012; 119:978–989. [PubMed: 22039261]
34. Cho H, Kehrl JH. Localization of Gi alpha proteins in the centrosomes and at the midbody: implication for their role in cell division. J Cell Biol. 2007; 178:245–255. [PubMed: 17635935]
35. Sauliere A, Bellot M, Paris H, Denis C, Finana F, Hansen JT, Altie MF, Seguelas MH, Pathak A, Hansen JL, Senard JM, Gales C. Deciphering biased-agonism complexity reveals a new active AT1 receptor entity. Nat Chem Biol. 2012; 8:622–630. [PubMed: 22634635]
36. Hwang IY, Hwang KS, Park C, Harrison KA, Kehrl JH. Rgs13 constrains early B cell responses and limits germinal center sizes. PLoS One. 2013; 8:e60139. [PubMed: 23533672]
37. Cyster JG, Schwab SR. Sphingosine-1-phosphate and lymphocyte egress from lymphoid organs. Annu Rev Immunol. 2012; 30:69–94. [PubMed: 22149932]
38. Sinha RK, Park C, Hwang IY, Davis MD, Kehrl JH. B lymphocytes exit lymph nodes through cortical lymphatic sinusoids by a mechanism independent of sphingosine-1- phosphate-mediated chemotaxis. Immunity. 2009; 30:434–446. [PubMed: 19230723]
39. Bansal G, DiVietro JA, Kuehn HS, Rao S, Nocka KH, Gilfillan AM, Druey KM. RGS13 controls g protein-coupled receptor-evoked responses of human mast cells. J Immunol. 2008; 181:7882–7890. [PubMed: 19017978]
40. Cho H, Harrison K, Schwartz O, Kehrl JH. The aorta and heart differentially express RGS (regulators of G-protein signalling) proteins that selectively regulate sphingosine 1- phosphate, angiotensin II and endothelin-1 signalling. Biochem J. 2003; 371:973–980. [PubMed: 12564955]
41. Hamdan FF, Percherancier Y, Breton B, Bouvier M. Monitoring protein-protein interactions in living cells by bioluminescence resonance energy transfer (BRET). Curr Protoc Neurosci. 2006; Chapter 5(Unit 5):23. [PubMed: 18428639]
42. Arnon TI, Cyster JG. Blood, sphingosine-1-phosphate and lymphocyte migration dynamics in the spleen. Curr Top Microbiol Immunol. 2014; 378:107–128. [PubMed: 24728595]
43. Melamed I, Wang G, Roifman CM. Antigen receptor-mediated protein tyrosine kinase activity is regulated by a pertussis toxin-sensitive G protein. J Immunol. 1992; 149:169–174. [PubMed: 1376748]
44. Blank JA, Clark GC, Wiegand G, Luster MI. Pertussis toxin inhibition of anti- immunoglobulin-stimulated proliferation and inositol phosphate formation. Toxicol Appl Pharmacol. 1990; 106:278–286. [PubMed: 2175054]
45. Anantharaman V, Abhiman S, de Souza RF, Aravind L. Comparative genomics uncovers novel structural and functional features of the heterotrimeric GTPase signaling system. Gene. 2011; 475:63–78. [PubMed: 21182906]

NIH-PA Author Manuscript

NIH-PA Author Manuscript

NIH-PA Author Manuscript

46. Lambert NA, Johnston CA, Cappell SD, Kuravi S, Kimple AJ, Willard FS, Siderovski DP. Regulators of G-protein signaling accelerate GPCR signaling kinetics and govern sensitivity solely by accelerating GTPase activity. Proc Natl Acad Sci U S A. 2010; 107:7066–7071. [PubMed: 20351284]
47. Zerangue N, Jan LY. G-protein signaling: fine-tuning signaling kinetics. Curr Biol. 1998; 8:R313–R316. [PubMed: 9560334]
48. Benians A, Nobles M, Hosny S, Tinker A. Regulators of G-protein signaling form a quaternary complex with the agonist, receptor, and G-protein. A novel explanation for the acceleration of signaling activation kinetics. J Biol Chem. 2005; 280:13383–13394. [PubMed: 15677457]
49. Zhong H, Wade SM, Woolf PJ, Linderman JJ, Traynor JR, Neubig RR. A spatial focusing model for G protein signals. Regulator of G protein signaling (RGS) protien-mediated kinetic scaffolding. J Biol Chem. 2003; 278:7278–7284. [PubMed: 12446706]
50. Jin T. Gradient sensing during chemotaxis. Curr Opin Cell Biol. 2013; 25:532–537. [PubMed: 23880435]
51. Garzon J, Rodriguez-Diaz M, Lopez-Fando A, Sanchez-Blazquez P. RGS9 proteins facilitate acute tolerance to mu-opioid effects. Eur J Neurosci. 2001; 13:801–811. [PubMed: 11207815]
52. Woolf PJ, Linderman JJ. Untangling ligand induced activation and desensitization of G-protein-coupled receptors. Biophys J. 2003; 84:3–13. [PubMed: 12524261]
53. Marchese A. Endocytic trafficking of chemokine receptors. Curr Opin Cell Biol. 2014; 27:72–77. [PubMed: 24680433]
54. Kang DS, Tian X, Benovic JL. Role of beta-arrestins and arrestin domain-containing proteins in G protein-coupled receptor trafficking. Curr Opin Cell Biol. 2014; 27:63–71. [PubMed: 24680432]
55. Kil LP, de Bruijn MJ, van Nimwegen M, Corneth OB, van Hamburg JP, Dingjan GM, Thaiss F, Rimmelzwaan GF, Elewaut D, Delsing D, van Loo PF, Hendriks RW. Btk levels set the threshold for B-cell activation and negative selection of autoreactive B cells in ice. Blood. 2012; 119:3744–3756. [PubMed: 22383797]

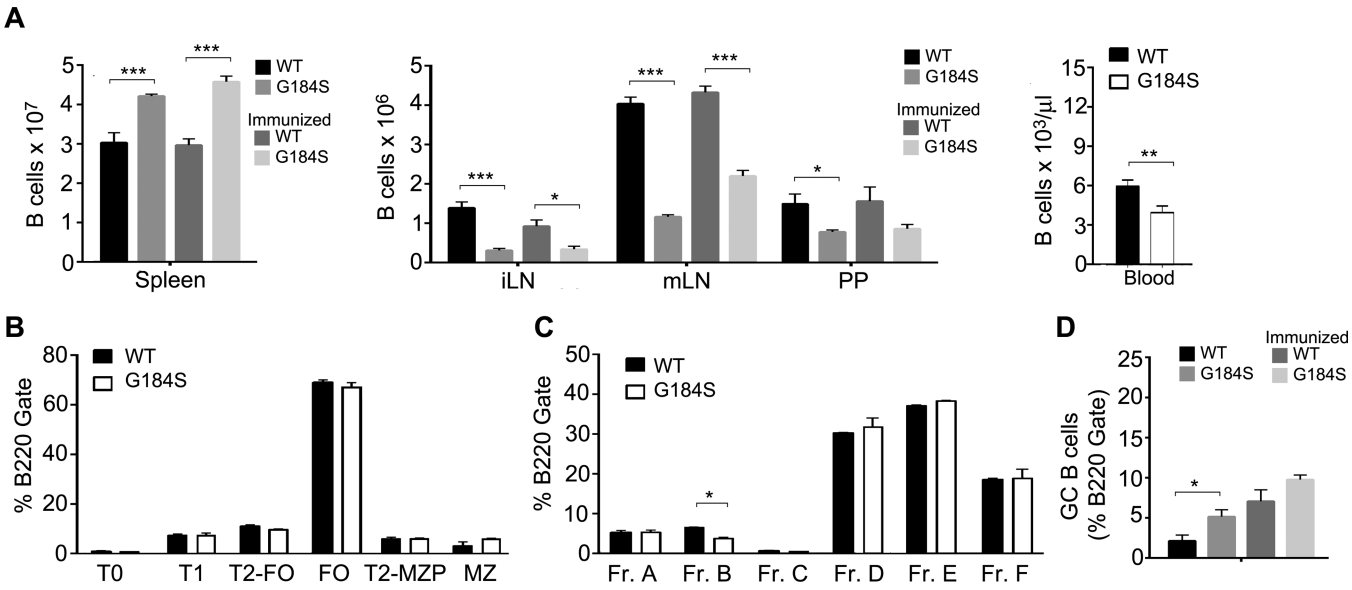

Figure 1.

Altered distribution of B cells in the lymphoid organs of G184S KI bone marrow chimeric mice. (**A**) Flow cytometric analysis to determine the number of B cells in the spleen, LNs, Peyer's patches and wild type and G184S KI bone marrow reconstituted mice immunized with sheep RBCs i.p (day 10) or not. Mice were analyzed 8–10 weeks after reconstitution. (**B**) Flow cytometric analysis of B cells from the spleen of bone marrow chimeric mice to examine splenic B cell development. (**C**) Flow cytometric analysis of B cells from the bone marrow of chimeric mice to examine B bone B cell development. (**D**) Flow cytometric analysis of splenic GC B cells from immunized or non-immunized bone marrow reconstituted mice. GC B cells defined as $B220^{+}CD38^{-}FAS^{+}GL7^{+}$. All experiments independently preformed 3 times with 3~4 mice and presented as the mean ± SEM of 3~4 mice per group.

NIH-PA Author Manuscript NIH-PA Author Manuscript NIH-PA Author Manuscript

NIH-PA Author Manuscript
NIH-PA Author Manuscript
NIH-PA Author Manuscript

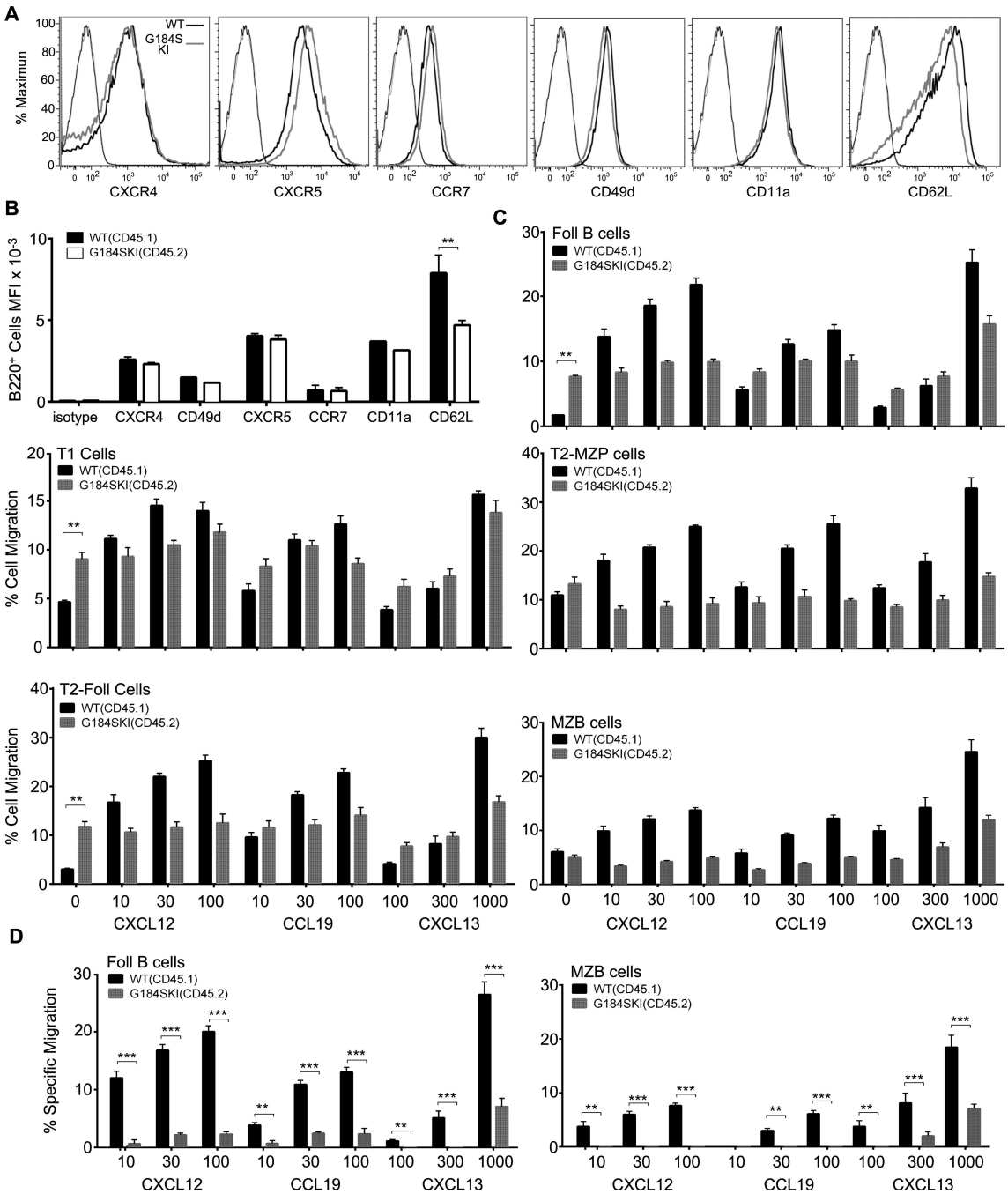

Figure 2.

G184S KI B cells have a severe defect in chemokine directed migration. (**A**) Flow cytometric analysis of B lymphocyte homing receptors using B cell purified from 3 wild type or 3 G184S KI bone marrow reconstituted mice. (**B**) Analysis of flow cytometry results from splenic B cells prepared from 5 wild type and 5 G184S KI mice. (**C**) Cell migration in chemotaxis assays used to evaluate the responses of splenic B cell subsets to CXCL12, CXCL13, and CCL19. B cells from six 1:1 mixed chimera mice were used and wild type and G184S KI B cells were distinguished on the basis of CD45.1 versus CD45.2 expression.

NIH-PA Author Manuscript

NIH-PA Author Manuscript

NIH-PA Author Manuscript

Data shown as the % cells migrated. Statistical differences are only shown for the non-specific migration. (**D**) Specific cell migration shown from chemotaxis assays evaluating the responses of follicular and marginal zone B cells. Specific migration is the amount of migration in the presence of chemokine minus the amount in the absence of chemokine. Statistical differences were calculated by 2- way ANOVA. Experiment repeated twice with similar results.

NIH-PA Author Manuscript

NIH-PA Author Manuscript

NIH-PA Author Manuscript

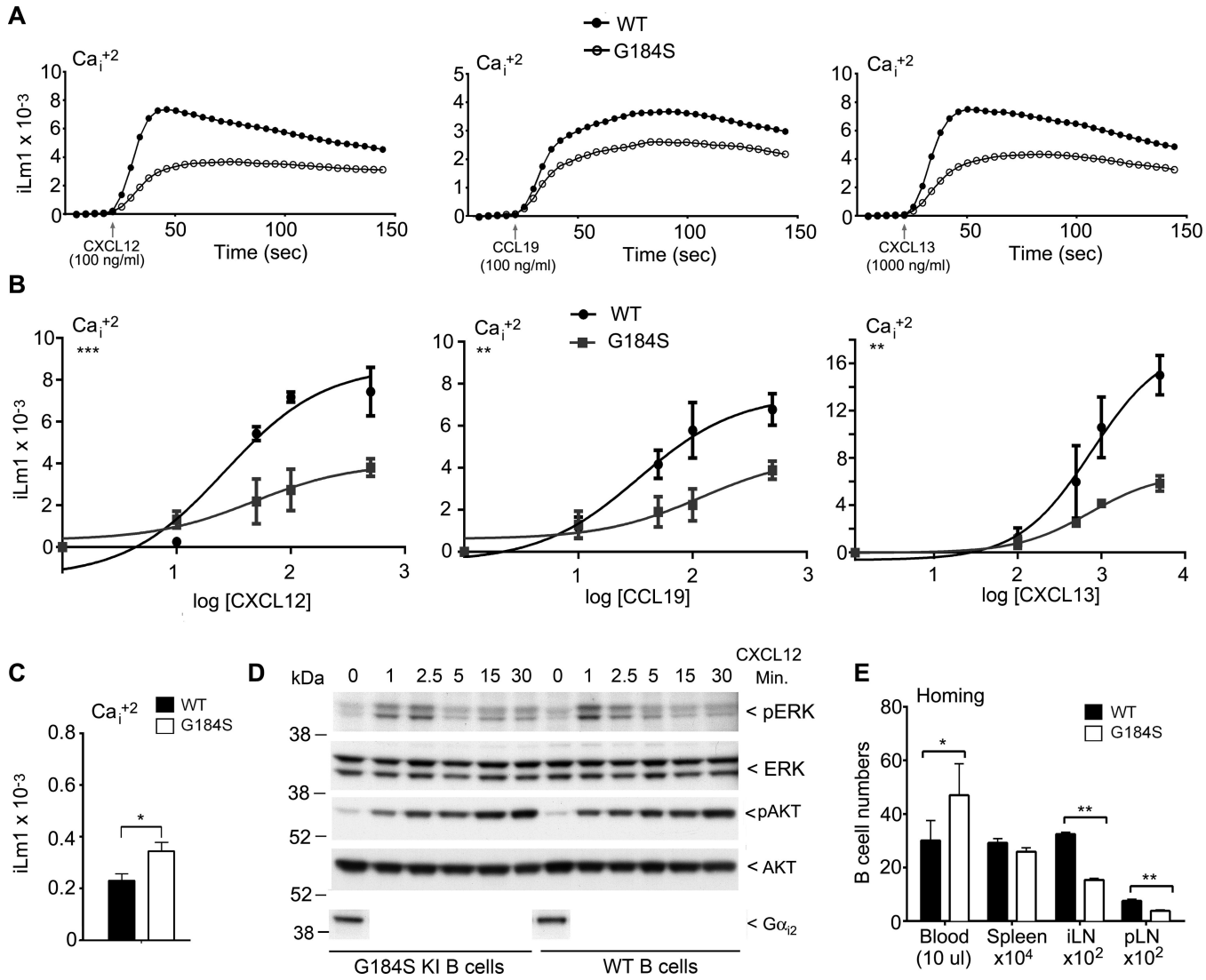

Figure 3.

G184S KI B cells have impaired chemokine receptor signaling and they home poorly to LNs. (**A**) Intracellular calcium response to near optimal chemokine concentrations using splenic B cells from wild type or G184S KI mice. The indicated chemokine and concentration used are shown. The results shown for each time point is the mean response from duplicate wells seeded with B cells from either wild type or G184S KI mice. Each experimental value is the mean of 2 determinations from 3 wild type and 3 G184S KI reconstituted mice. Assay was done duplicate per mouse. The basal levels of calcium were used to normalize the responses. (**B**) Peak intracellular calcium plotted as a function of the log concentration of the indicated chemokine concentration. Results from 3 wild type and 3 G184S KI reconstituted mice performed in duplicate. Data shown as mean +/− standard error of the mean. A non-linear regression curve fit generated using Prism software. Statistical differences calculated by one-way Anova. (**C**) Analysis of Intracellular calcium levels in non-stimulated wild type and G184S KI B cells prepared in from 3 wild type and 3 G184S KI bone marrow reconstituted mice. Data shown as mean +/− standard error of the

NIH-PA Author Manuscript

NIH-PA Author Manuscript

NIH-PA Author Manuscript

mean. Statistical differences calculated by unpaired *t* test. (**D**) Immunoblotting for pERK, total ERK, pAKT, and total AKT in B cell lysates from B cell stimulated with CXCL12 (100 ng/ml). The B cells were prepared from 2 wild type and 2 G184S KI reconstituted mice. Fold change is shown. (**E**) Results from a 2 hour homing assay. B cells prepared from 3 wild type and 3 G184S KI bone marrow reconstituted mice were labeled and injected intravenously into 6 wild type mice. The numbers of cells in the blood, spleen, popliteal LN, and the inguinal LNs were determined by flow cytometry. Experiment performed three times with similar results. Data shown as mean +/− standard error of the mean. Statistical differences calculated by *t* test.

NIH-PA Author Manuscript
NIH-PA Author Manuscript
NIH-PA Author Manuscript

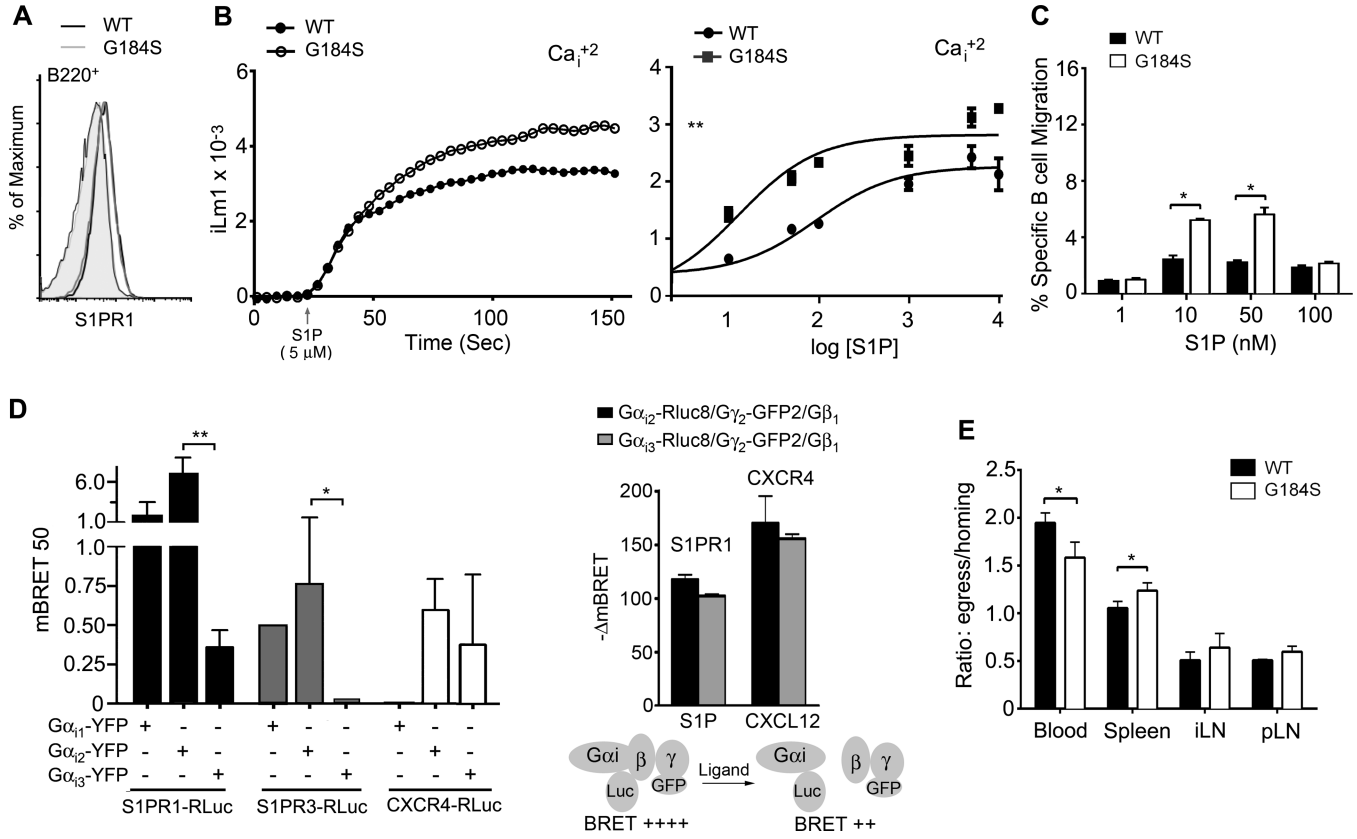

Figure 4.

G184S KI B cells have augmented S1P receptor signaling and no obvious impairment in LN egress. (**A**) Flow cytometry of B220+ B cells from WT and G184S KI mice to examine S1PR1 expression levels. Left two profiles (overlapping) are the background controls and the right two profiles (overlapping) are the S1PR1 antibody reactivity. (**B**) Intracellular calcium response to S1P using either wild type or G184S KI B cells. A representative calcium response to S1P stimulation is shown in left panel. In the right panel the peak intracellular calcium levels were plotted as a function of the log concentration of the S1P concentration used. Results from 2 wild type and 2 G184S KI reconstituted mice performed in duplicate. Data shown as mean +/− standard error of the mean. A non-linear regression curve fit generated using Prism software. (**C**) Cell migration in chemotaxis assays used to evaluate the responses of splenic B cells S1P. B cells from the 1:1 mixed chimera mice were used and wild type and G184S KI B cells were distinguished on the basis of CD45.1 versus CD45.2 expression. Data shown as the % cells migrated. Statistical differences calculated by 2- way ANOVA. (**D**) BRET assay to analyze the affinity of S1PR1, S1PR3, and CXCR4 for $G\alpha_i$ proteins and $G\alpha_i$ activation. HeLa cells expressing a BRET donor (S1PR1-RLuc, S1PR3-RLuc, or CXCR4-RLuc) and increasing amounts of the construct coding for BRET acceptor ($G\alpha_{i1}$ -YFP, $G\alpha_{i2}$ -YFP, or $G\alpha_{i3}$ -YFP). The BRET ratios were calculated and the change in BRET determined (left panel). HeLa cells expressing either S1PR1 or CXCR4 along with the indicated plasmids were stimulated with S1P (200 nM) or CXCL12 (200 ng/ml) and changes in mBRET were measured. (**E**) Comparison of wild type and G184S KI B cell egress. B cells were prepared from 2 wild type, and from 2 G184S KI bone marrow

NIH-PA Author Manuscript

NIH-PA Author Manuscript

NIH-PA Author Manuscript

reconstituted mice. The B cells were differentially labelled, mixed 1:1, and injected intravenously into 8 wild type mice. At 2 hours after injection 4 mice were sacrificed and 4 mice received CD62L. The later mice were sacrificed 18 hours later. The numbers of transferred cells in the spleen, inguinal LN, popliteal LN, and the blood was determined by flow cytometry. The data shown is the ratio between the cells at 18 hours and 2 hours at the different sites. Experiment repeated twice with similar results.

NIH-PA Author Manuscript
NIH-PA Author Manuscript
NIH-PA Author Manuscript

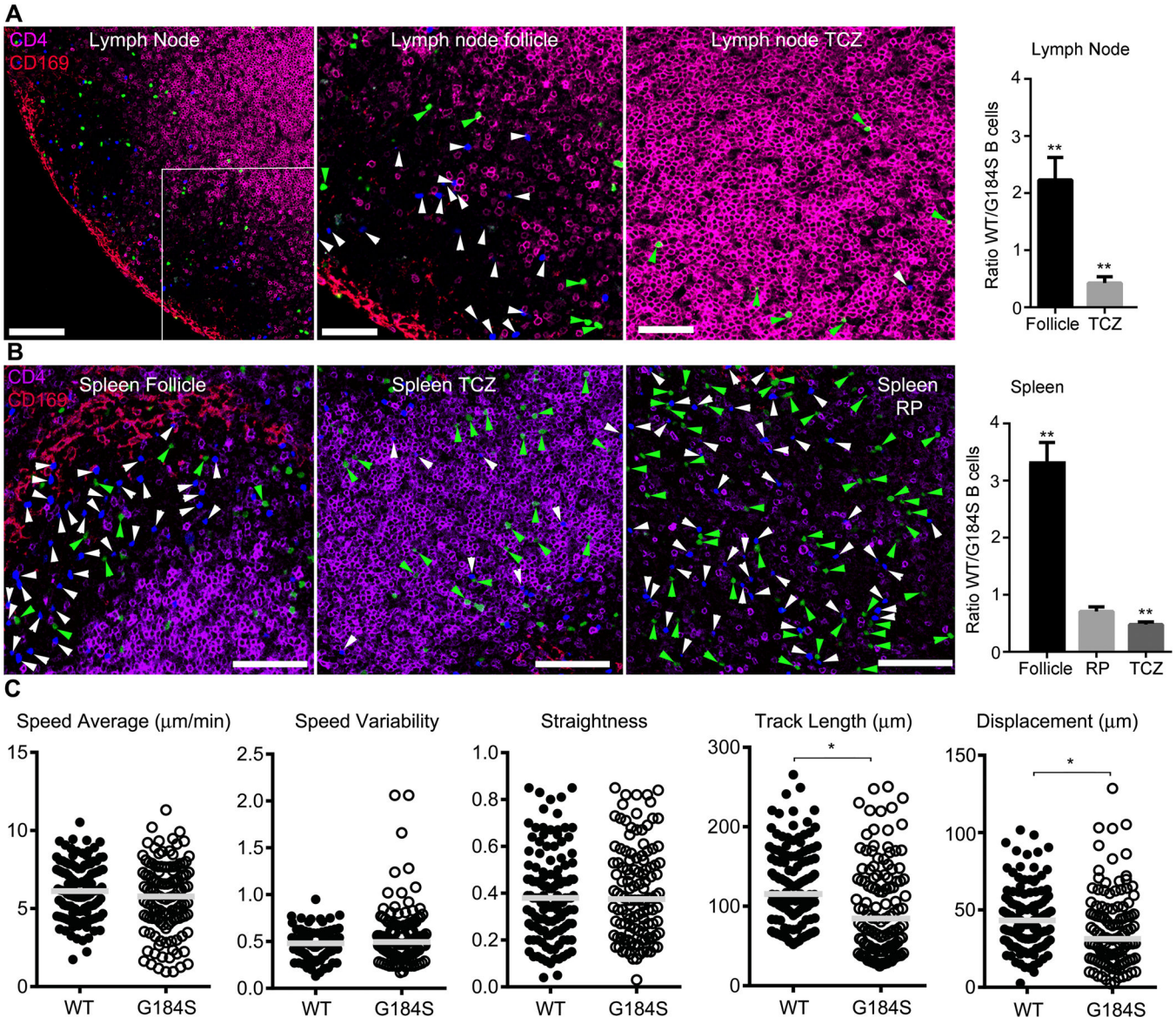

Figure 5.

Impaired G184S KI B cell positioning in the spleen and LNs, but relatively normal motility. (**A & B**) Confocal microscopy to identify the location 24 hours after their adoptive transfer of wild type and G184S KI B cells in the inguinal LNs (A) or spleen (**B**). The location of wild type (blue) and G184S KI B cells (green) in sections immunostained for CD69 and CD4 are shown in the left panels and 4× zoomed image of the indicated regions are shown in the middle and right images. The ratios of wild type (WT) to G184S KI B cells in the indicated sites are shown in the graphs on the right. TCZ- T cell zone; RP- red pulp. From left to right the scale bars are 100, 50, and 50 μm, top image, and all 100 μm, lower image. (**C**) Results from the intravital two photon imaging of the inguinal LN of a mouse that served as the recipient for adoptively transferred wild type and G184S KI B cells that had been differentially labeled. Cell tracking and analysis performed using Imaris software. Two

imaging experiments were performed with similar results. Statistical differences calculated by *t* test.

NIH-PA Author Manuscript
NIH-PA Author Manuscript
NIH-PA Author Manuscript

NIH-PA Author Manuscript
NIH-PA Author Manuscript
NIH-PA Author Manuscript

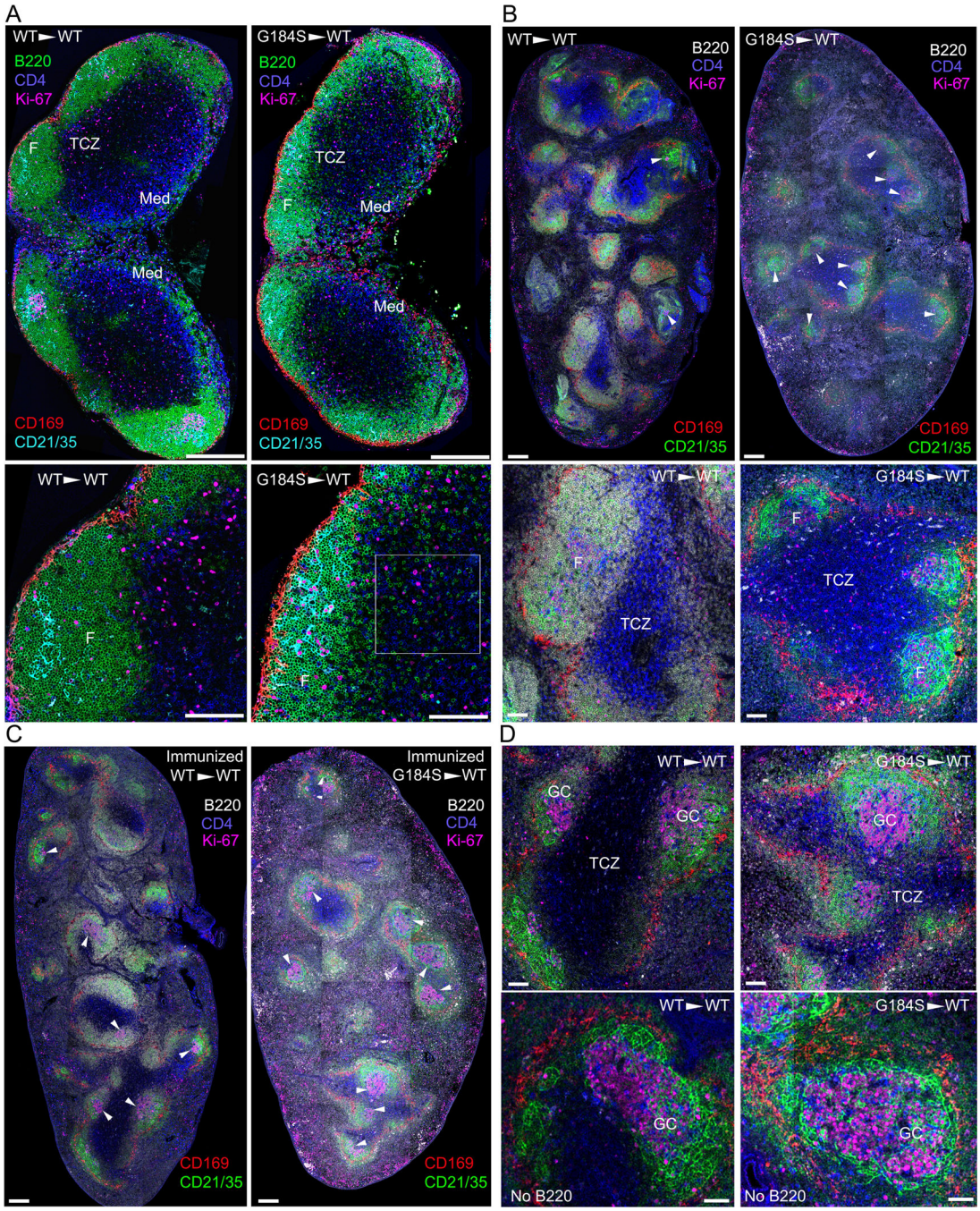

Figure 6.

Small LN follicles and spleen B cell follicles in the G184S KI mice. (A) Confocal microscopy of the inguinal LN of a wild type and a G184S KI bone marrow reconstituted mice. LNs were fixed and immunostained with directly fluorescently labeled antibodies recognizing B220 (green), CD4 (blue), Ki67 (pink), CD169 (red), and CD21/35 (turquoise). The images were tiled to reconstruct an image of the entire LN. Shown below are 3× electronic magnification focused on one of the LN follicles (F) and the adjacent T cell zone (TCZ). Boxed area shows numerous G184S KI B cells located in the TCZ. Scale bars are

NIH-PA Author Manuscript

NIH-PA Author Manuscript

NIH-PA Author Manuscript

300 μm (top) and 100 μm (bottom). (B) Confocal microscopy of the spleens from a wild type and a G184S KI bone marrow reconstituted mice. A thick splenic section was fixed and immunostained with directly fluorescently labeled antibodies recognizing B220 (white), CD4 (blue), Ki67 (pink), CD169 (red), and CD21/35 (green). The images were tiled to reconstruct an image of the entire spleen. GCs are indicated with white arrowheads. Shown below are 4× electronic magnification focused on the splenic white pulp. The splenic B cell follicle (F) and T cell zone (TCZ) are indicated. Scale bars are 400 μm (top) and 100 μm (bottom). (C & D) Confocal microscopy of spleens from a wild type and a G184S KI bone marrow reconstituted mice immunized 10 days previously with sheep RBCs. A thick splenic section was fixed and immunostained with directly fluorescently labeled antibodies recognizing B220 (white), CD4 (blue), Ki67 (pink), CD169 (red), and CD21/35 (green). The images were tiled to reconstruct an image of the entire spleen (C). GCs are indicated with white arrowheads. Scale bars are 400 um. Electronic zoomed images (D) are shown on the right. In the bottom images the B220 signal was removed to allow better visualization of the GC structure. The T cell zone (TCZ) is indicated. Scale bars are 100 μm.

NIH-PA Author Manuscript

NIH-PA Author Manuscript

NIH-PA Author Manuscript

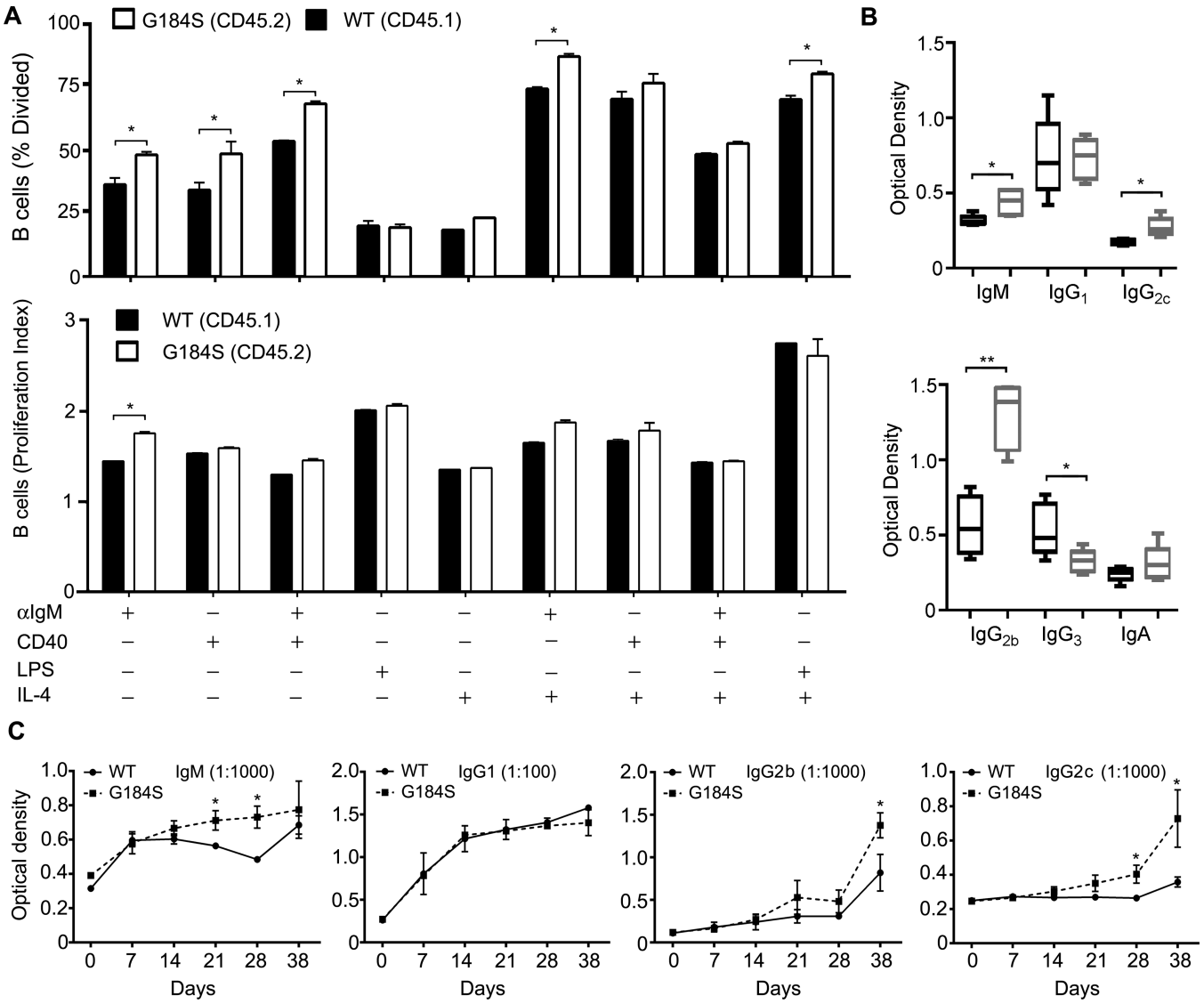

Figure 7.

Increased G184S KI B cell division in response to BCR crosslinking and abnormal humoral responses in G184S KI mice. (**A**) CFSE dye dilution assay to assess B cell proliferative responses to different inductive signals. Splenic B cells were purified from mice previously adoptively transferred with a 1:1 mix of wild type and G184S KI bone marrow. The B cells were stimulated with the indicated reagents for 4 days and CFSE dilution patterns were assessed by flow cytometry. The results were used to calculate the % of cells that divided and a proliferative index for each condition. The wild type and G184S KI B cells were distinguished by CD45.1 versus CD45.2 expression. (**B**) Serum immunoglobulin levels in wild type and G184S KI mice. Total serum levels were measured by ELISA. (**C**) Specific antibody response to TNP-KLH immunization. Wild type and G184S KI mice were immunized with TNP-KLH with alum via intraperitoneal injection. Pre-immune and weekly serum samples were collected for 4 weeks. Afterwards the mice were boosted via intraperitoneal injection. Serum was collected 1 week later. Specific IgM and IgG isotype

levels were measured by ELISA using plates coated with TNP-BSA. Statistical differences were calculated by *t* test.

NIH-PA Author Manuscript
NIH-PA Author Manuscript
NIH-PA Author Manuscript